BNL 36421

Proceedings - Conference on Autoionization of Atoms and Small Molecules
Argonne National Laboratory, May 2-3, 1985

PHOTOELECTRON STUDIES OF AUTOIONIZING RYDBERG STATES IN HCl

M. G. White and J. R. Grover
Chemistry Department, Brookhaven National Laboratory
Upton, NY 11973

BNL--36421

DE85 011813

ABSTRACT

The results of a systematic investigation of electronically autoionizing Rydberg states in HCl are discussed. Vibrationally resolved photoelectron spectroscopy was used to map out the non-radiative decay of vibronic levels of $3p\sigma \rightarrow n(\begin{matrix}s\\d\end{matrix})\sigma$ Rydberg states converging to the $A^2\Sigma^+(3p\sigma)^{-1}$ excited ionic state. The observed vibrational distributions of the resulting $X^2\Pi(1\pi)^{-1}$ ionic state are compared with the results of model calculations of Terwilliger and Smith based on spectral analysis of the absorption spectrum. Overall, the $X^2\Pi$ vibrational branching ratios are found to be in only rough qualitative agreement with the calculations and these results are discussed in relation to the approximations involved.

INTRODUCTION

Unlike Rydberg series involving promotion of the outermost valence electron, Rydberg states resulting from excitations of deeper lying valence orbitals usually lie above the ionization potential. Although the latter belong to the neutral excited state manifold, such "super-excited" Rydberg levels are likely to interact with the degenerate ionization continuum, leading to the well-known phenomenon of autoionization. Autoionizing Rydberg and non-Rydberg resonances have been identified and characterized for a large number of molecules by photoabsorption and photoionization (integrated) measurements.[1] Their effect on the internal energy distribution of the resulting ions, however, has been difficult to study due to the lack of suitably intense laboratory light sources (below 1000 Å) required for such detailed, differential measurements. With the increasing availability of intense and continuously tunable VUV radiation from synchrotron radiation facilities, such studies are now quite feasible and photoelectron studies of electronic autoionization in several molecules have been reported.[2,3,4] In addition to photoelectron spectroscopy, ionic state fluorescence excitation spectra[5,6] and fluorescence polarization measurements[7] using dispersed synchrotron radiation sources are also proving to be effective and complimentary probes of molecular autoionization. By characterizing the final state distribution of the compound system, i.e., molecular ion and ejected photoelectron, these experimental methods can provide the physical insight and quantitative data for development and evaluation of theoretical models of molecular autoionization.

In this work we present exemplary results of a photoelectron spectroscopy study of electronically, autoionizing Rydberg series in small molecules recently begun at the National Synchrotron Light Source (NSLS). Particular emphasis has been placed on characterizing the systematics of the autoionizing series by following individual decay channels as functions of the parameters which specify a given molecular Rydberg state, i.e., n, ℓ, λ and the molecular ion core α, v_α (α and v_α are the electronic and vibrational quantum numbers describing the molecular ion core, respectively). Hydrogen chloride was chosen as an ideal initial system for several reasons; (i) the photoabsorption[8] and photoionization[9] curves for HCl are rich in well-resolved autoionizing lines whose width (autoionization lifetime induced) is large (~500 cm^{-1}) relative to the bandwidth (80-100 cm^{-1}) of the excitation source; (ii) the lower members of these autoionizing series ($3p\sigma \rightarrow n\ell\sigma$) form well separated vibrational series, so that autoionization can be followed as a function of n and v_α; (iii) the vibrational levels of the $X^2\Pi$ ground ionic state to which these Rydberg levels decay can be readily resolved; (iv) Terwilliger and Smith[10] have provided a theoretical prediction of the HCl^+ photoelectron spectra for resonant excitation via the P(I), v = 0 - 4 Rydberg states based on an analysis of the photoabsorption spectrum. The model calculations, mentioned above also provide an opportunity to judge the validity of assumptions involved in the qualitative analysis of photoelectron spectra following resonant excitation, e.g., the Franck-Condon approximation.

EXPERIMENTAL

The experiments were carried out on the U-11 beam line on the VUV storage ring at the National Synchrotron Light Source. A 4-meter, normal incidence monochromator in a modified-Wadsworth configuration[11] is used to provide intense, tunable VUV radiation in the wavelength range 350 Å - 2000 Å. Using a 3600 ℓ-mm^{-1} grating, a photon bandwidth of 0.5 Å - 1.0 Å was obtained, depending on the vertical size of the stored electron bunch in the VUV ring. Focussed radiation was intercepted after the exit slit and channeled to the photoelectron spectrometer via a 2 mm (ID) glass capillary light guide which provides a highly effective gas barrier between the spectrometer and the UHV environment of the beam line. Photoelectrons produced at the intersection of the VUV radiation and an effusive gas jet and ejected into a 3.5° angular cone are collected and energy analyzed by a hemispherical analyzer (50 mm mean radius) set for a 5 eV pass energy. For the HCl studies presented here, the analyzer was fixed at the "magic angle" (~55°) appropriate for 100% linearly polarized light. Latter measurements on other molecular systems were taken with the analyzer mounted on a fully rotatable turntable which was set to a "magic angle" (~61°)[12] determined by the linear polarization measured by a Rabinowitz-type

polarization analyzer (~ 63%).[13] The difference in "magic angle" positions can lead to systematic errors in the partial cross sections for HCl of 10-15% depending on the asymmetry parameter (β) for a particular vibronic channel. Such uncertainties are not large enough, however, to effect the basic quantitative comparisons discussed here. Photoelectron spectra are normalized to the light intensity and corrected for the transmission of the electron analyzer as determined from calibration runs with He and Ne.

RESULTS AND DISCUSSION

The photoionization spectrum of HCl^+ in the resonance spectral region near the $A^2\Sigma^+(3p\sigma)^{-1}$ excited state threshold at 762.8 Å is shown in Fig. 1. This curve was obtained on the U-11 beam line at 0.5 Å resolution with a molecular beam photoionization mass spectrometer described elsewhere.[14] Comparison with previous room temperature photoabsorption[10] and the -150°C photoionization[9] spectra shows no significant narrowing of the broad P(I),v resonances centered near 830 Å as might be expected from rotationally "cold" HCl produced in the 800 Torr supersonic expansion. This suggests that the

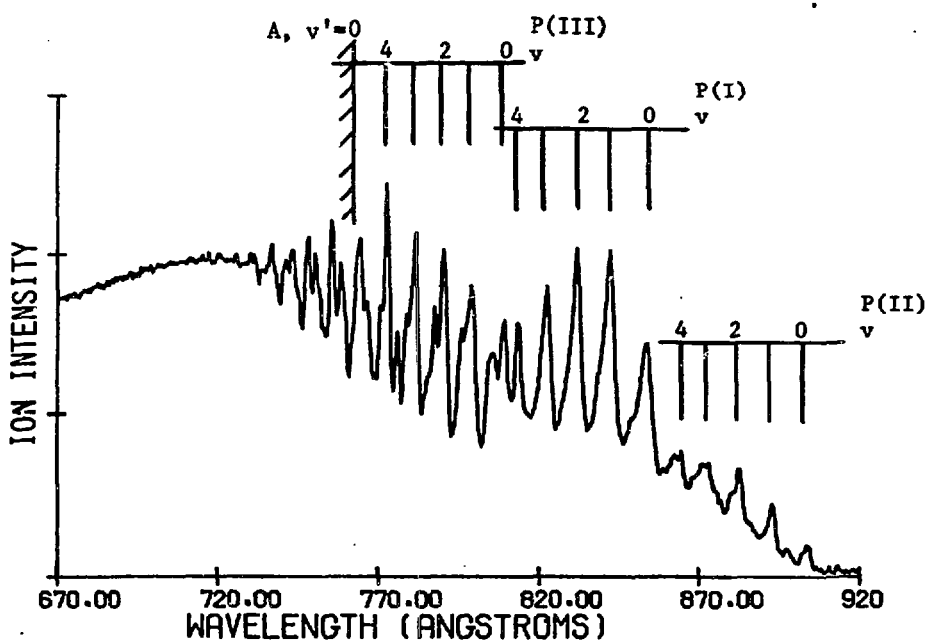

Fig. 1. Photoionization spectrum of HCl^+ near the $A^2\Sigma^+(3p\sigma)^{-1}$ threshold.

non-radiative lifetime is much greater than the rotational spacing and is consistent with the complete lack of observable rotational structure in the high resolution absorption spectrum.[8] The n and v_α assignments are based on the spectral analysis of Terwilliger and Smith,[8,10] however, a complete symmetry assignment was not possible due to the absence of rotational structure. From plausibility arguements these authors assign the P(I) and P(III) vibronic series to $n(\pi_d^e)\sigma\ ^1\Sigma^+$ symmetry with $n^* = 2.795$ and $n^* = 3.795$, respectively, while the weaker P(II) vibronic series is assigned to an unresolved $np(\pi^\sigma)$ complex with $n^* = 2.31$.

Resonant and non-resonant photoelectron spectra of HCl are shown in Fig. 2. The lower, non-resonant spectrum was taken at a photon energy of 584 Å (HeI) at which the photoionization cross section shows no discrete structure and is well above the ionization energy of the $A^2\Sigma^+(3p\sigma)^{-1}$ excited ionic state. The extended vibrational envelope of the $A^2\Sigma^+$ state is consistent with the known increase in bond length (+.24 Å) relative to the neutral ground state resulting from the removal of a bonding $3p\sigma$ electron. From the expected similarity of the Rydberg state potential curves and that of $A^2\Sigma^+$ state to which they converge, simple Franck-Condon arguements would suggest that autoionization via Rydberg vibronic levels will lead to extensive vibrational excitation of the $X^2\Pi$ ionic ground state. Such a resonant spectrum is shown in the upper part of Fig. 2 corresponding to excitation of P(III), v = 1 resonance at 792.7 Å. Enhanced vibrational excitation of the resulting ion is clearly evident with significant populations in vibrational levels with $v' > 1$.

Since all of the Rydberg states are expected to have very similar potential curves to that of the $A^2\Sigma^+$ ionic state, it was of considerable interest to examine the vibrational energy distribution of the ion following autoionization for a fixed Rydberg state geometry, i.e., same v_α. Such results bear on the general validity of employing the Franck-Condon approximation in molecular electronic autoionization. According to the model developed by Terwilliger and Smith[10] to describe autoionization in the hydrogen halides, the intensity of a vibrational level of the $X^2\Pi$ state of the ion v' following excitation of a Rydberg state with vibrational quantum number v_α is given by

$$\sigma(v_\alpha,v') = \sigma_T^e \left[F_{v'v''} + F_{v'v_\alpha} \cdot F_{v_\alpha v''} \cdot \rho_e^2(q_e)^2\right] \qquad (1)$$

where σ_T^e is the electronic part of the direct, total photoionization cross section, F_{ij} are Franck-Condon factors between vibrational levels i and j, v'' is the vibrational level of the neutral ground state (v'' = 0), q_e is the electronic line profile and the product, $F_{v_\alpha v''} \cdot \rho_e^2(q_e)^2$ is proportional to the autoionization peak height. In addition, this model assumes that the autoionization resonance width is larger than the excitation bandwidth and rotational width and that the excitation energy is tuned to the resonance peak maximum. Both requirements are met for the present HCl experiments. This theoretical model

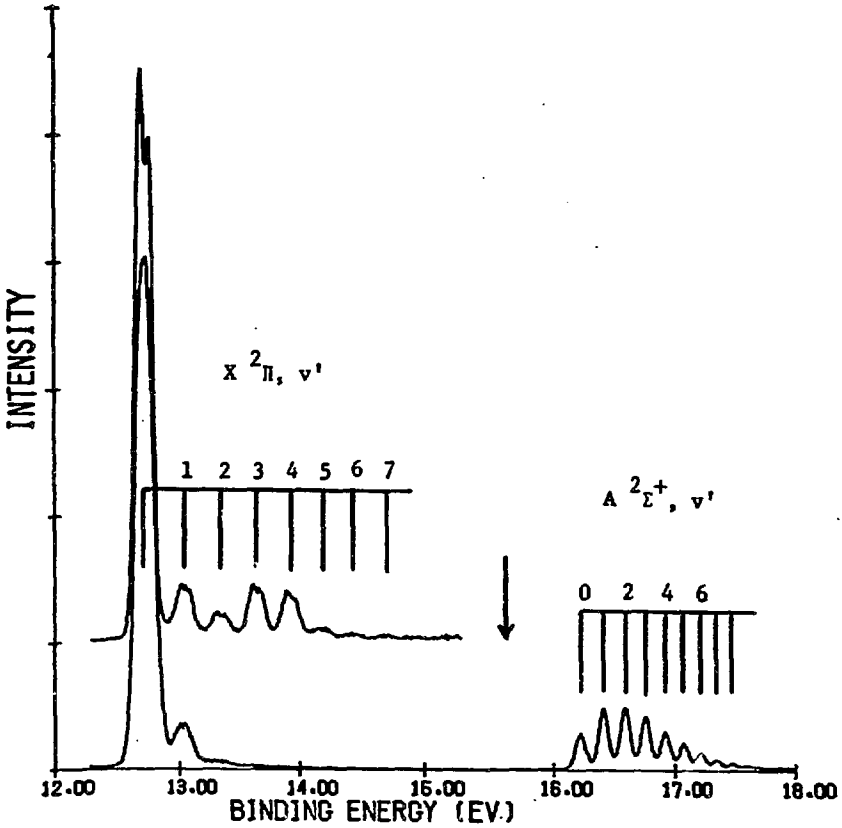

Fig. 2. Resonant (upper) and non-resonant (lower) photoelectron spectra of HCl. The lower spectrum was taken at 584 Å while the upper spectrum corresponds to resonant excitation of the P(III), v=1 Rydberg state at 792.7 Å. The arrow indicates the energy position of this resonance. The doublet observed in the $X^2\Pi$, v'=0 line in the upper, resonant spectrum results from the partially resolved $^2\Pi_{1/2}$ and $^2\Pi_{3/2}$ spin-orbit components (72 meV separation) of the HCl^+ ground state.

is similar to other previous simplified approaches to characterizing the vibrational distribution of the ion following electronic autoionization.[15,16] From this expression we note that if the geometry factors are frozen, i.e., same v" and v_α, the ionic state vibrational intensities are dependent only on $F_{v'v_\alpha}$ and the product of the electronic terms $\rho_e^2(q_e)^2$

which Terwilliger and Smith[10] note are independent of n*. Photoelectron spectra relevant to this latter point are given in Figs. 3 and 4. These spectra correspond to resonant excitation of the v = 1 and v = 2 levels of the P(I) and P(III) Rydberg states which belong to the same series but differ in n by one. For the v_α = 1 Rydberg states the $X^2\Pi$ vibrational distributions are quite similar with a secondary maximum at v' = 3. In the v_α = 2 case, the overall $X^2\Pi$ vibrational distributions are alike, i.e., both have minima at v' = 3, however, the vibrational populations relative to the v' = 0 level are quite different, particularly for v' = 1 and 2. Although differences in the P(I) and P(III) spectra could be attributed to differences in their respective potential curves, it is unlikely that such large differences in the v_α = 2 spectra can be accounted for this way.

Additional tests of eqn (1) can be made by comparing the predicted $X^2\Pi$ vibrational branching ratios of the P(I),v_I Rydberg levels with experiment. Terwilliger and Smith[10] used parameterized fits of the P(I),v_I resonance profiles in the absorption spectrum to obtain values for the product $F_{v_I v''}\rho_e^2(q_e)^2$ which were used to predict photoelectron spectra via eqn (1). The results are summarized in Table 1. Overall, the quantitative agreement with experiment is poor, with the theoretical calculations over estimating the contribution of autoionization induced vibrational excitation relative to the direct process. This can be partly traced to the difficulty noted by Terwilliger and Smith[10] of establishing the relative contributions of the direct and resonant cross sections and suggest that the autoionization contribution is overestimated in their calculations. On a qualitative basis, the vibrational distributions predicted for the P(I),v_I = 0,1,2 resonances are in reasonable agreement with experiment. For the P(I),v_I = 3 and 4 resonances, however, maxima and minima are displaced in v' relative to experiment. These latter results may reflect inadequacies in determining the Franck-Condon factors $F_{v'v_I}$ which become more sensitive the the parameters used to describe the Rydberg state potential curve as v_I increases.

Overall, comparison of the Franck-Condon model of Terwilliger and Smith[10] gives a roughly qualitative description of the autoionizing Rydberg series in HCl. Several improvements including examining the Franck-Condon factors for $v_I > 2$ and changing the relative contributions of the direct to resonance cross sections, which changes the magnitude of the $F_{v_\alpha v''}\rho_e^2(q_e)^2$ term, could most likely improve the quantitative comparison without rejecting the basic approximations involved. Whether the disagreement of the model calculations and experiment suggest the breakdown of the Franck-Condon approximation or even more extreme, the Born-Oppenheimer approximation, remains to be further addressed in additional work on HCl and other diatomic systems. In this context it should be

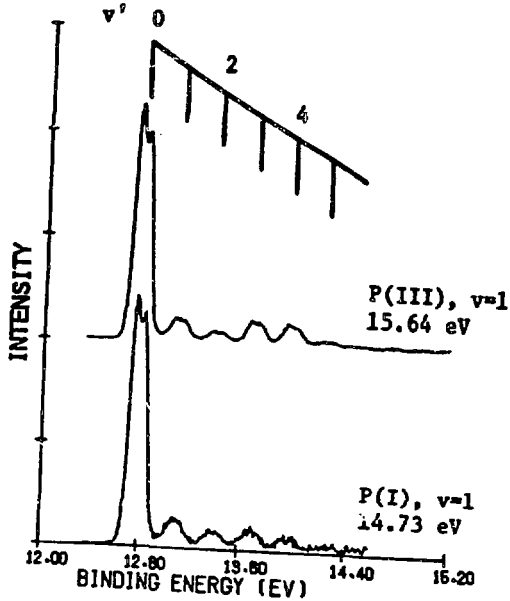

Fig. 3. Resonant HCl photoelectron spectra for v=1 levels of the P(I) and P(III) Rydberg states.

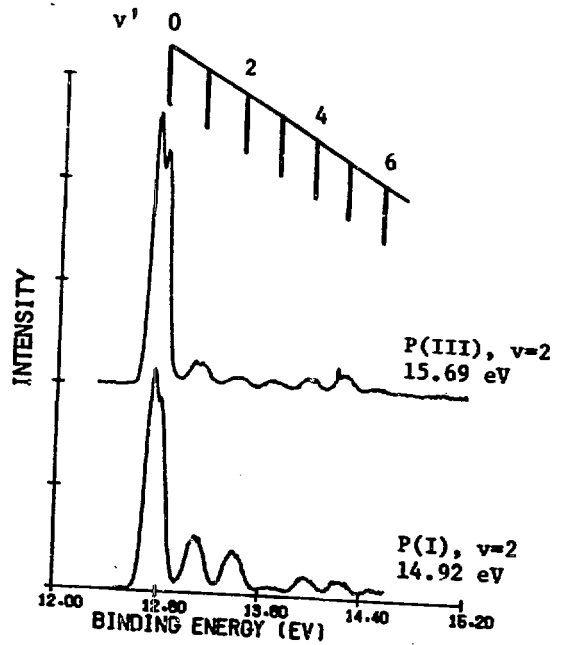

Fig. 4. Resonant HCl photoelectron spectra for v=2 levels of the P(I) and P(III) Rydberg states.

noted that in the recent photoelectron study of electronic autoionization in CO, Ederer et al.,[17] found that the observed ionic state vibrational distributions are very roughly given by Franck-Condon factors between the Rydberg state and final ionic state, $F_{v'v_a}$. Aside from additional experimental studies, the importance of retaining the R-dependence in the electronic interaction matrix elements ($\langle \frac{1}{r_{12}} \rangle$) will most likely be determined from newer, fully ab initio theoretical treatments of the autoionization process such as multichannel quantum defect theory (MQDT). To date, the only such ab initio MQDT calculation addressing specifically electronic autoionization, i.e., the Hopfield series of N_2,[18] does not include R-dependence in the MQDT electronic quantities or calculate ionic state vibrational intensities. Such future theoretical investigations will certainly add a great deal more to our overall understanding of electronic autoionization in molecules.

ACKNOWLEDGEMENT

This research was carried out at Brookhaven National Laboratory under contract DE-AC02-76CH00016 with the U. S. Department of Energy and supported by its Division of Chemical Sciences, Office of Basic Energy Sciences.

REFERENCES

1. J. Berkowitz, Photoabsorption Photoionization and Photoelectron Spectroscopy (Academic, New York, 1979).
2. J. L. Dehmer, D. Dill and A. C. Parr, "Photoionization Dynamics of Small Molecules", Photophysics and Photochemistry in the Vacuum Ultraviolet, edited by S. McGlynn, G. Findley and R. Huebner (D. Reidel Publishing Co., Dordrecht, Holland, 1983) and references therein.
3. M. J. Hubin-Franskin, J. Delwiche, P. Morin, M. Y. Adam, I. Nenner and P. Roy, J. Chem. Phys. 81, 4246 (1984).
4. P. Morin, I. Nenner, M. Y. Adam, M. J. Hubin-Franskin, H. Lefebvre-Brion and A. Guisti-Suzor, Chem. Phys. Lett., 92, 609 (1982).
5. H. Hertz, H.-N. Jochims and W. Sroka, J. Phys. B 1, 548 (1974).
6. K. Ito, A. Tabché-Fouhailé, H. Frohlich, P. M. Guyon and I. Nenner, J. Chem. Phys. 82, 1231 (1985) and references therein.
7. E. D. Poliakoff, J. L. Dehmer, A. C. Parr and G. E. Leroi, J. Chem. Phys. 77, 5243 (1982).
8. D. T. Terwilliger and A. L. Smith, J. Mol. Spectrosc. 45, 366 (1973).
9. P. M. Dehmer and W. A. Chupka, Radiological and Environmental Research Division Annual Report, Argonne National Laboratory, 1978, #ANL-78-65, p. 13.

10. D. T. Terwilliger and A. L. Smith, J. Chem. Phys. 63, 1008 (1975).
11. M. R. Howells, Nucl. Instrum. Methods 195, 215 (1982).
12. J. A. R. Samson and A. F. Starace, J. Phys. B8, 1806 (1975).
13. J. A. R. Samson, Rev. Sci. Instrum. 47, 859 (1976).
14. M. G. White and J. R. Grover, J. Chem. Phys. 79, 4124 (1983).
15. A. L. Smith, Phil. Trans. Roy. Soc. (London) A268, 169 (1970).
16. J. L. Bahr, A. J. Blake, J. H. Carver, J. L. Gardner and V. Kumar, J. Quant. Radiat. Transfer 11, 1839 (1971); 12, 59 (1972).
17. D. L. Ederer, A. C. Parr, B. E. Cole, R. Stockbauer, J. L. Dehmer, J. B. West and K. Codling, Proc. Roy. Soc. (London) A378, 423 (1981).
18. M. Raoult, H. LeRouzo, G. Raseev and H. Lefebvre-Brion, J. Phys. B16, 4601 (1983).

Table I Vibrational Branching Ratio

$X^2\Pi, v'$ / $P(I), v_I$	0	1	2	3	4	5	6	7
0								
Theory[a]	6.87(-1)[b]	1.85(-1)	9.02(-2)	3.07(-2)	6.44(-3)			
Experiment	7.7(-1)	1.4(-1)	5.8(-2)	2.9(-2)	7.7(-3)			
1								
Theory	6.23(-1)	4.14(-2)	6.28(-2)	1.41(-1)	9.52(-2)	3.09(-2)		
Experiment	7.7(-1)	7.5(-2)	4.8(-2)	6.1(-2)	3.4(-2)	1.7(-2)		
2								
Theory	5.78(-1)	6.40(-2)	7.12(-2)	2.00(-4)	8.36(-2)	1.24(-1)	6.25(-2)	
Experiment	6.2(-1)	1.5(-1)	1.1(-1)	5.0(-3)	4.8(-2)	4.4(-2)	2.5(-2)	
3								
Theory	5.98(-1)	1.03(-1)	4.79(-3)	4.64(-2)	2.13(-2)	1.85(-2)	9.81(-2)	8.08(-2)
Experiment	6.8(-1)	1.6(-1)	4.9(-2)	4.5(-2)	1.7(-2)	7.0(-3)	2.1(-2)	2.1(-2)
4								
Theory	6.78(-1)	9.30(-2)	1.17(-2)	2.24(-2)	7.08(-3)	3.37(-2)	—	4.92(-2)
Experiment	6.8(-1)	1.7(-1)	3.8(-2)	2.5(-2)	3.8(-2)	3.2(-2)	—	7.4(-2)

[a] Reference (10).

[b] Values written as 6.87(-1) are to read 6.87×10^{-1}.

DISCLAIMER